Structural efficiency metrics for integrated selection of layup, material, and cross-section shape in laminated composite structures

Haichao An [a, b], Singh Jasveer [b], Damiano Pasini [b,*]

[a] School of Astronautics, Beihang University, XueYuan Road No.37, HaiDian District, 100191 Beijing, China

[b] Department of Mechanical Engineering, McGill University, Montreal, QC H3A 0C3, Canada

Abstract:

Previously introduced to assess the structural efficiency and to ease the selection of solid materials and cross-section shapes, the method of shape transformers is here extended to deal with the structural design of laminated composites. In particular, this work examines laminated composites under bending and torsional loading, and considers as free variables of selection the layup, the number of plies, the shape of the cross-section, and the materials that make up a laminated structure. Structural efficiency measures are first formulated to assess the merit of selecting each of these variables separately, and later applied to generate design charts that enable their concurrent selection. The results visualized in maps help identify in a glance the role that each of the variables plays in the structural efficiency of a laminated composite structure, as well as assist in the choice of the best laminated composite concept at the preliminary stage of design.

Keywords: Material selection charts; Performance indices; Selection for composite materials

1. Introduction

With the recent advent of automated processes for composite manufacturing, the use of laminated composites is steadily increasing and stretching its potential with applications stemming from a large spectrum of sectors, including aerospace, marine, and land. In general, fiber orientations, stacking sequence, and laminate thickness are some, among several others, design variables that can be rationally optimized to obtain laminated structures with excellent mechanical properties at minimum mass.

The design of a single laminate is generally less challenging than the design of a structure, like a cantilever, made of composite laminates. In this case, besides the stacking sequence, other design variables, such as the cross-section shape and the overall form of the structure, can be chosen as design variables to achieve a performance improvement. In a composite laminated structure with constant stiffness, variables governing its specific stiffness and strength include the fiber orientation in each layer, the layup, the constituent materials of each layer as well as the cross-sectional shape of the structure. Since some of the material-related variables are

* Corresponding author. Tel: +1 514 398 6295; Fax: +1 514 398 7365. E-mail: damiano.pasini@mcgill.ca.

directional and their interaction with the structural variables can be strong, the structural design of laminate composites can often present higher complexity than that with conventional materials. Thence, design tools of selection can be handy at the concept stage of design as they can assist in making educated choices on the design variables that can best maximize structural efficiency in a given application.

A number of approaches have been proposed for material and shape selection of monolithic or hybrid materials [1]-[3]. One of the most popular is the pioneering method of Ashby, which was first introduced for the selection of monolithic shaped materials via performance indices, and then it was extended to hybrid materials [4]-[6], with fibrous composites being an example [7]. More recently, in the context of composite materials, Buckney et. al [8] presented shape factors to measure the structural efficiency of beam cross-sections under asymmetric bending, and applied them to a cross-section composed of multiple materials. Another work that provides metrics for ranking alternative design configurations for composites is that of Thomas and Qidwai [9], who used material-architecture indices to quantitatively correlate system-level performance of discrete composite components to that of their constituent properties describing material and geometry. While effective in providing design tools of selection for multiple material components, the works above do not examine the layup of a composite laminate and thus are of limited use in the choice of the layup for a laminated composite structure.

With respect to the layup design of a laminate composite, tools for layup selection exist and carpet plots are one example [10]. Carpet plots allow to find an appropriate laminate layup for given load conditions and mechanical requirements. Carpet plots illustrate how a given laminate property depends on the percentage of plies at each orientation. Carpet plots are handy to use and can thus offer a convenient tool for the early stage selection of the laminate layup. Later, such plots were used and extended by Weaver [11] in a work for layup selections of composite structures, where a database of laminate layup was developed to store the properties of all permutations of layup angles. A series of maps presented to search a subset of laminates that perform well on each chart, allows to visually identify trends of properties that might otherwise be overlooked by using numeric methods. Building upon Weaver's methodology [11], more recently Monroy Aceves et al. [12] combined the use of FE analysis with the selection software CES [13] to help designers select a shortlist of composite structures from a large number of options. These charts give freedom to modify the selection criteria and design requirements to allow interactive selection of data. The methodology was also applied to a real case study, requiring the design of a small low-speed composite wind turbine blade [14], showing its suitability in identifying the most promising concept for a composite blade. Whereas the works mentioned above focus on the layup and/or material selection in shell or plates made of composite materials, the interaction between cross-section shape, material and layup in laminated composite selection has not been examined yet and it is thus the focus of this paper.

In this work, we extend a method previously introduced for material and shape selection of lightweight structures [15]-[18]. It is based on the definition of shape

transformers, dimensionless measures that can be defined for any geometric properties of a structure, such as its volume. Shape transformers describe shape properties regardless of size and material, and are thus invariant to any scaling imposed to the size of a structure. The method allows to distinctly capture the role of cross-section shape and material in the structural properties and structural efficiency of a structure. Previously used for the co-selection of shaped materials in single and multi-objective applications [15]-[18], the method is here extended to integrate information on the layup, making it capable of handling the design and selection of laminated composite structures. In Section 2, the paper starts by reviewing the fundamentals of the method before focusing on extending the formulation to obtain performance indices for laminated composite beams. In section 3, the developed indices are used to generate selection charts showing the role of cross-section shapes material properties and layup in bending and torsional stiffness design. Selection charts for bending and torsional strength design are also presented in Section 4, which is followed by concluding remarks.

2. Methodology

2.1 A brief review of the concept of shape transformers

Introduced for solid materials and applied to problems of selection for lightweight design [19], vibration[15], and biological beams [20], shape transformers have been formulated for a range of loading scenarios including stiffness and strength in pure bending [16][21], torsion stiffness [18], and combination of bending and shear [17].

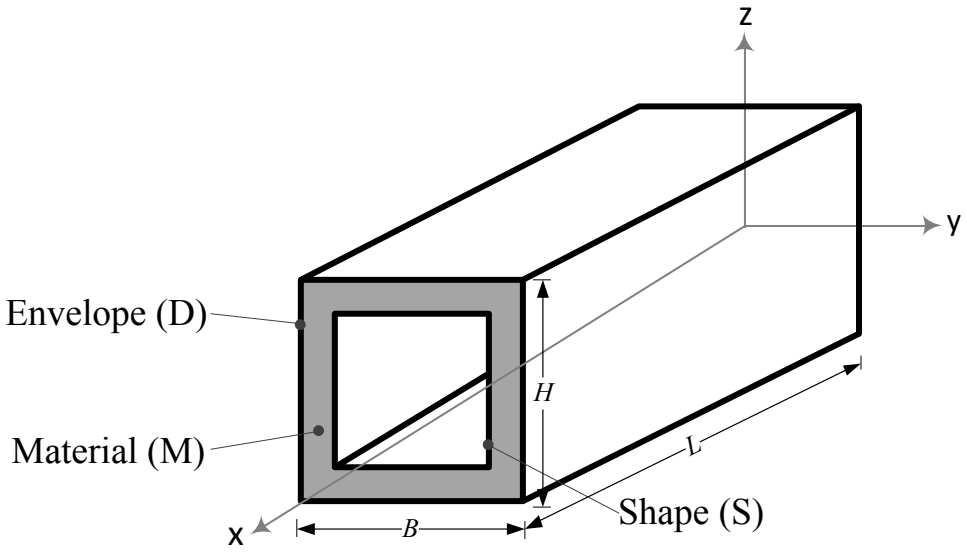

Fig. 1 Hollow prismatic beam made of a uniform homogenous material with its design variables (M, S, D)

For a given prismatic structure, such as that shown in Fig.1, we can conveniently assume the structural properties to be dependent on the material (M) it is made of, the shape (S) of its cross-section, and the overall size, here conveniently described by the rectangular envelope (D) with dimensions (H), (B) and (L). As material properties allow comparing materials for a given envelope D, similarly we can define shape

properties, namely shape transformers, that are normalized with those of the envelope and are thus dimensionless. Shape transformers can be defined for the area, volume, second moment of area and other given geometric quantities (G) of a structure, so as to be invariant to scaling. For a given cross-section, a shape transformer (Ψ_{G}) of a geometric quantity G is defined by normalizing the geometric quantity G by the same geometric quantity of its envelope G_D, such that $\Psi_{\mathrm{G}} = \mathrm{G}/\mathrm{G}_D$. For example, $\Psi_A = A/A_D$ is the shape transformer of area, where A is the area of the cross-section and A_D is the area of the envelope.

Table 1 shows a summary of the performance indices containing shape transformers that were formulated to measure the structural efficiency of a cross-section in stiffness and strength designs under bending and torsional loadings. On the upper part there are indices for solid materials [15]-[18], whereas in the lower part are those that are derived in the next section of this work for laminated composites.

Table 1 Performance indices for conventional solid materials and composite laminates. *u=B/Bo* and *v=H/Ho* describe relative changes in size between a reference baseline envelope (B_0, H_0, L_0) and that (B, H, L) of the structure which the baseline is compared to. If the envelope is prescribed *u=v=*1, which corresponds to the case examined in this work for laminated composites. E, G and ρ are the Young's modulus, shear modulus and material density, respectively, and σ_{f} and τ_{f} are the material strengths in bending and torsion, respectively. $\mathrm{M_f}$ and $\mathrm{T_f}$ are the critical failure bending moment and torsion torque, and Ψ_{I} and Ψ_{JT} are the shape transformers for bending and torsion.

Material type	Cross-section scaling	Loading case	Stiffness	Strength
Solid materials	Arbitrary scaling	Bending	$\frac{(E\Psi_I)^q}{\rho\Psi_A}$ $(q = \frac{\ln uv}{\ln uv^3})$	$\frac{(\Psi_I\sigma_f)^q}{\rho\Psi_A}$ $(q = \frac{\ln uv}{\ln uv^2})$
		Torsion	$\frac{(G\Psi_{JT})^q}{\rho\Psi_A}$ $(q = \frac{\ln uv}{\ln u^{1.55}v^{2.45}})$	$\frac{(\Psi_{JT}\tau_f)^q}{\rho\Psi_A}$ $(q = \frac{\ln uv}{\ln u^{1.55}v^{1.45}})$
	Prescribed envelope	Bending	$\frac{E\Psi_I}{\rho\Psi_A}$	$\frac{\Psi_I\sigma_f}{\rho\Psi_A}$ *or* $\frac{M_f}{\rho\Psi_A}$
		Torsion	$\frac{G\Psi_{JT}}{\rho\Psi_A}$	$\frac{\Psi_{JT}\tau_f}{\rho\Psi_A}$ *or* $\frac{T_f}{\rho\Psi_A}$
Laminated composites	Prescribed envelope	Bending	$\frac{\Psi_{EI}}{\rho\Psi_A}$	$\frac{\Psi_{M_f}}{\rho\Psi_A}$
		Torsion	$\frac{\Psi_{GJ}}{\rho\Psi_A}$	$\frac{\Psi_{T_f}}{\rho\Psi_A}$

2.2 Extension of the definition of shape transformers to laminated composites

Whereas Fig. 1 shows a prismatic beam of solid materials, Fig. 2 shows its counterpart beam made of composite laminates, the object of our study. Variables we focus here our attention on, are (M, S, θ, n), where M is the material of each ply, S the

cross-section shape, θ and n the ply angle of each layer and the number of plies. The size of the structure, namely the envelope D, is prescribed. With convention following the right-hand-rule, the x-axis is the beam axis and the beam cross-section is in the y-z plane. In this work we examine the stiffness in the z-direction. Further work is required to generalize the analysis to other directions.

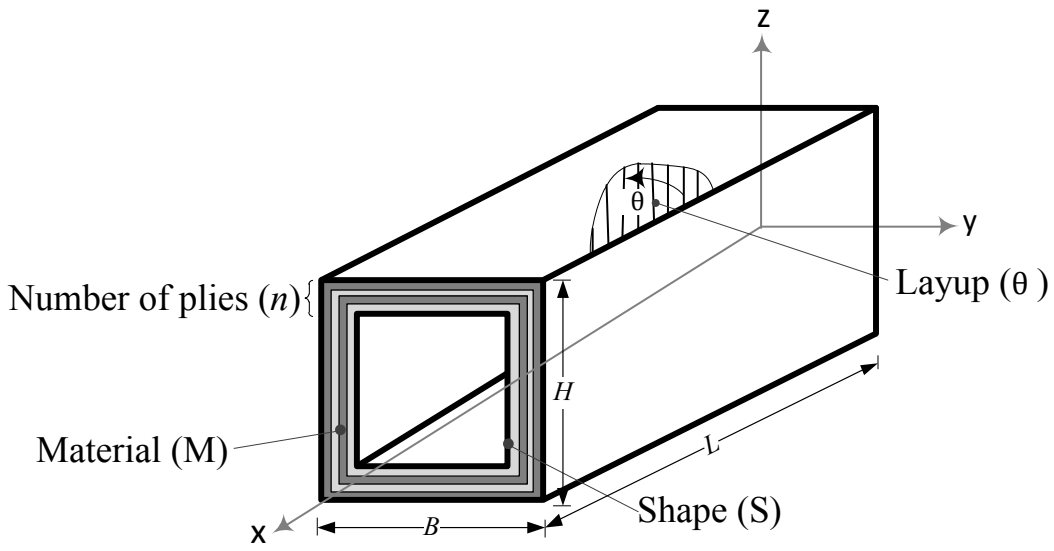

Fig. 2 A composite laminated beam with emphasis on the variables (M, S, θ, n) considered in this work

Whereas for solid materials the role of material and shape could be conveniently decoupled in the formulation of the performance indices [15]-[18], for laminated composites there exists a intrinsic interaction between material, shape, and layup, variables that are thus are difficult to decouple, as seen from the formulations derived in [22]. For this reason, the performance indices for laminated composites are here defined for stiffness and strength design as a bending index (Ψ_{EI}) which is the ratio of bending stiffness of a candidate cross-section normalized to the reference cross-section. For the reference cross-section, the beam is made of composite materials, and its cross-section shape, number of plies and ply angle for each layer can be specified according to the design references and requirements. In this work, as later described in Section 3, we refer to a reference cross-section with square box shape, 16 plies and 0° degree of angle for all layers made of E-Carbon Epoxy (CFRP). With this information on the reference cross-section, we can define the bending stiffness index as

$$\Psi_{EI} = \frac{EI}{(EI)_0} \tag{1}$$

Similarly, the torsional stiffness index

$$\Psi_{GJ} = \frac{GJ}{(GJ)_0} \tag{2}$$

where the subscript "$_o$" indicate the properties of the reference cross-section.

Similarly a mass index can be defined as $\Psi_{\rho A} = \rho A/(\rho A)_0$. But since the material density in the product ρA can be decoupled from the cross-sectional area, the mass index corresponds to the respective shape transformer defined for conventional solid materials.

In terms of strength, a set of performance indices need to be defined for laminate composites. Due to the strong interaction between the design variables and the ply stress as well as the complexity in choosing an appropriate failure criterion for laminate composites, we define a composite index for bending strength as Ψ_{M_f}. Expressed in terms of the critical failure moments, this index is given by the ratio of the critical bending failure moment of a candidate cross-section and that of the reference cross-section as

$$\Psi_{M_f} = \frac{M_f}{(M_f)_0} \tag{3}$$

And for torsional strength design, the corresponding index is defined as

$$\Psi_{T_f} = \frac{T_f}{(T_f)_0} \tag{4}$$

We note that the shape transformer indices defined above for composite laminates depend on the material, cross-section shapes as well as layup, as opposed to those for conventional materials, which depend on the cross-section shape only, due to the uncoupling existing between material and geometry.

We now use the indices defined in Eqs.(1)-(4) to formulate performance indices for stiffness and strength designs in bending and torsion loading conditions. In this work, we focus on laminate composite structures of given size, i.e. the envelope is prescribed, thereby leaving material, shape, and layup as active variables of selection. For a given envelope, the performance index of a cross-section for bending stiffness design can be written with respect to that of the reference cross-section as

$$P = \frac{\Psi_{EI}}{\rho \Psi_A} \tag{5}$$

Similarly, for torsional stiffness design, the performance index is defined as

$$P = \frac{\Psi_{GJ}}{\rho \Psi_A} \tag{6}$$

A third performance index is formulated to compare the performances in bending and torsion simultaneously, which can be suitable to plot selection charts for maximum bending and torsional stiffness. This is expressed as

$$P = \frac{\Psi_{EI}}{\Psi_{GJ}} \tag{7}$$

A high value of the performance index in Eq.(7) indicates the candidate cross-section performs better in bending than in torsion.

For strength, similar to the case of conventional solid materials (see Eq.(A.18) in

Appendix A), the bending strength index of performance is given for a candidate cross-section with respect to a reference cross-section (of given size) by

$$P = \frac{\Psi_{M_f}}{\rho \Psi_A} \tag{8}$$

Similarly, for torsion strength design (see Eq.(A.21) in Appendix A), the index is

$$P = \frac{\Psi_{T_f}}{\rho \Psi_A} \tag{9}$$

To measure the strength in bending relative to that in torsion, we can define

$$P = \frac{\Psi_{M_f}}{\Psi_{T_f}} \tag{10}$$

This index is useful to produce selection charts for maximum bending and torsional strength, as shown in a later section of this paper. A high value represents cross-section performing better in bending than torsion for strength. The lower part of Table 1 summarizes the performance indices for composite laminates; and Appendix B shows the derivation of the critical loadings that are used in the expressions of the shape transformers and performance indices presented above.

We note that the indices for laminate composites become identical to those for conventional materials if the reference cross-section is assumed to be solid and if the properties of the materials in the ply are non-directional. In this case, the structure becomes a multimaterials system identical to that described in [15], where the material and the geometry were uncoupled. Hence the indices defined here are more general and can model all the cases previously examined with this method.

3. Selection charts for bending and torsional stiffness design

In this section, we apply the performance indices presented above to four types of composite laminated beams (Fig.3) with material properties given in Table C.1 (Appendix C). The size of each beam cross-section is specified, i.e. the envelope is given. The goal is to examine different combinations of layup, cross-section and materials, by using the indices to first assess their structural efficiency and then illustrate how they can be of aid in developing design maps of selection.

To develop selection charts, we consider here a demonstrative design scenario, i.e. a cantilever beam, although the results here presented can be extended to other design cases with other geometric parameters and layup attributes for the beam. Given here are the size of the cross-section, i.e. the envelope, with B=50mm and H=50mm, and the length equal to L=0.5m. The lay-up under investigation here are orthotropic, as these are commonly used in laminate composite design. We recall that to make any laminate orthotropic, one can either use only 0 and 90 degree plies, or use a balanced laminate in which plies of positive and negative angles are placed adjacent to each other. These laminates can be represented as,

Angle Ply: $[\theta \quad -\theta \quad \theta \quad -\theta \ ...]$

Cross Ply: [0 90 0 90 ...]

For demonstrative purposes, here we also assume that the laminate beams have a number of plies that can vary from 0 to 24. In addition, the reference cross-section is appropriately selected to be a square box, with 16 plies and 0° degree of angle for all layers made of E-Carbon Epoxy (CFRP).

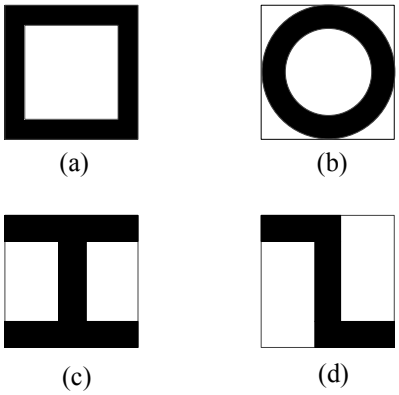

Fig. 3 Standard sections used in this work as demonstrative application for the development of selection charts for laminate composites. (a) Hollow square or square box, (b) Hollow cylinder or tube, (c) I-beam, (d) Z-beam.

3.1 Selection charts for minimum mass and maximum bending stiffness

In laminated composite design a common goal is often to seek for values of the design variables that can provide minimum mass and maximum bending stiffness. These two objectives are strictly in conflict. Hence, often the need for numeric analysis is felt even at the conceptual stage. The design charts presented in this work aim at bypassing this step of numeric analysis by providing readily available charts that assist in selecting separately and concurrently the best combination of (M, S, θ, n). To do so in the following sections, we proceed by activating the design variables gradually: first M and S are given, leaving (θ, n) as variables, then S becomes active and variables are (S, θ, n), and finally (M, S, θ, n) as variables of selection.

3.1.1 Co-selection of shape and layup

In this scenario, where the material properties are given and the active variables are cross-section shape and layup, the performance index reduces to

$$P = \frac{\Psi_{EI}}{\Psi_A} \tag{11}$$

Fig.4 shows a plot of the bending index, i.e. the numerator of Eq. (11), on the y-axis, versus the shape transformer of the area, i.e. its denominator, on the x-axis. The results are obtained from closed-form expressions for laminate composites [22]. Each point on this chart represents a design configuration for a square box with varying ply angle and number of plies. For a given material, in this case CFRP, the boundaries of the triangular domain represent the potential for the angle ply of a laminate beam with square box shape; in particular the domain informs of all possible configurations a layup can offer for a ply angle ranging from 0 to 90^o (i.e. from A to B) and number of plies from 0 to 24 (from O to A). For example, consider a case where the designer has

to compare the performance of a cross-section having 20 plies with ±20° layup, indicated as P on the chart, with other candidate layups. From this chart, we can infer that this layup is 0.8 times stiffer and 1.25 times heavier than the reference cross-section (a CFRP square box with 16 plies and 0 degree of angle for all layers), which is given by $\Psi_{EI} = \Psi_A = 1$ and represented by a horizontal line. A number of other useful insights can be directly gained from the chart. For example, there exist an infinite number of designs that have the stiffness equal to the one of the reference cross-section, but the reference-cross-section is the lightest. Yet, depending upon the application, a designer may be inclined towards selecting a design with 24 plies at ±20° (denoted as Q on the chart), as this layup may meet the required level of shear stiffness. In this case, it is the trade-off between mass and shear stiffness that needs to be assessed since the bending stiffness is equal for both designs.

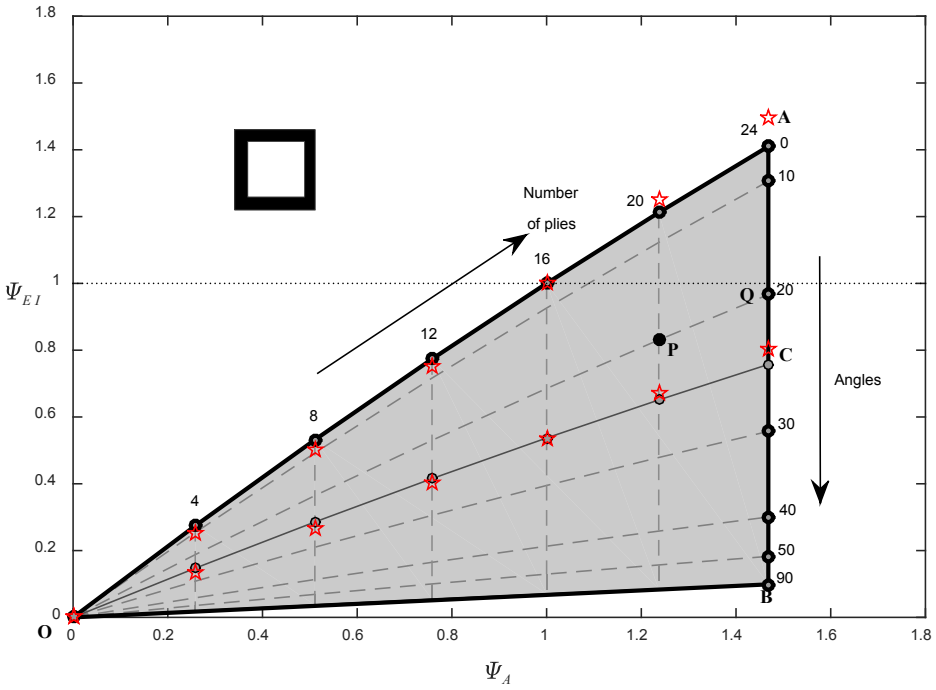

Fig. 4 Design chart for the selection of ply angle and number of plies for a given square box. (Red stars indicate numerical results obtained from FEA)

Whereas all the charts presented in this paper are obtained from closed-form expressions [22], we emphasize that numeric simulations have been carried out for validation purposes using a commercial finite element software (MSC.Patran/Nastran, Newport Beach, CA). To avoid overcrowding the maps, however, the validation points in this work are reported for two cross-section shapes only, i.e. the square box section (closed cross-section) and the I-beam section (open cross-section), (Fig.4 above and Fig.5 below, respectively). For each finite element simulation, a proper mesh size, convergence and accuracy were ensured for elastic analysis. Concerning the boundary conditions, the cross-section was assumed to be free to warp so as to be able to retrieve the numerical values of the warping constant given in [22]. The maximum difference between the numeric and analytic results is found to be for all

cases below 6%, a value that originates from the approximations made in deriving the constants. Nevertheless, this accuracy is deemed acceptable especially for the conceptual stage of design.

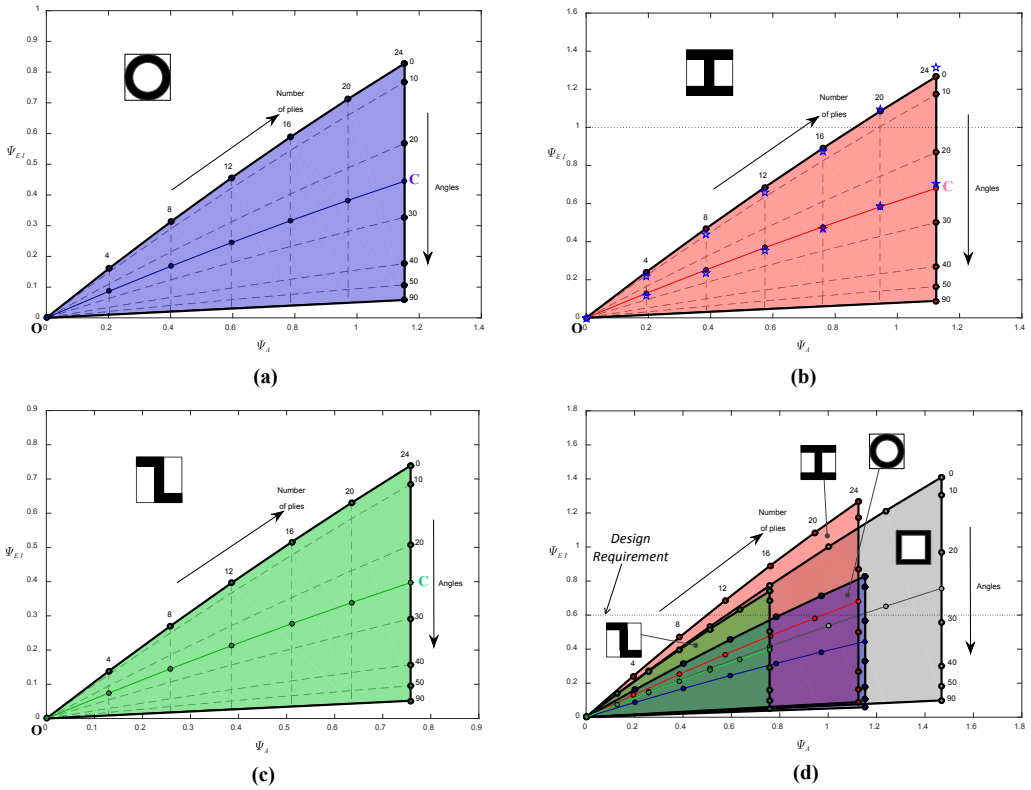

Fig. 5 Design charts for the selection of shape and layup for a prescribed material. (Blue stars represent FEA obtained solutions; cross-angle designs are shown in thin solid lines, i.e. from O to C)

While Fig. 4 is plotted for a square box, the bending stiffness efficiency is plotted in Fig. 5(a) to 5(c) respectively for the other cross-section shapes examined in this work (Fig. 3), with given material and beam size. Fig. 5(d) illustrates all of them on a single chart that allows the concurrent comparison of cross-section shape and lay-up. Looking at the top boundary of each domain, we observe that the tube cross-section has the lowest slope and hence is the least efficient, followed by the Z-beam and square box sections. The I-beam performs best. The overall extents of their domain, however, change. By simply inspecting the chart, we can infer that if one wishes to replace a square box section with a tube one, the number of plies should increase by more than 1.5 times, thus increasing the mass by 30%. Also, for a given shape, the 0° angle ply gives the best performance in bending. This is due to the different behaviors of a laminate, which strictly depends on the fiber direction: composite layers are much stiffer in the fiber direction than in the perpendicular direction. In addition, the performance decreases gradually as the angle increases from 0 to 10 degrees and then deteriorates sharply from 10 to 40 degrees. Thereafter, the performance decrease becomes gradual again. Quantitatively, the decrease can be measured from their respective slopes. This chart also aids in interpreting the performance of a cross-ply

laminate with respect to the angle ply. For instance, for a given shape and number of plies, a cross-ply laminate (indicated by thin lines on the chart, i.e. from O to C) performs equally in bending as angle ply with the angle around 24°.

As a further example demonstrating the use of these charts, consider a design problem in which the stiffness requirement is given and depicted by a dotted horizontal line in the co-selection chart of Fig. 5d. There are infinite cross-sections that fulfill the stiffness requirement prominent among which are (a) I-beam, 0° angle ply, 12 plies; (b) Square box, 0° angle ply, 12 plies; (c) Z-beam, 0° angle ply, 20 plies; (d) Tube, 0° angle ply, 16 plies; (e) I-beam, cross ply, 20 plies; (f) Square box, cross ply, 20 plies. These designs are arranged in accordance to their performance (mass). Since the relative performance can be measured directly from the chart, the designer can choose one of the listed cross-sections depending upon other criteria, such as a given shear stiffness requirement, and manufacturing issues among others. It can also be seen that a tubular cross-ply cannot fulfill this requirement.

3.1.2 Co-selection of material, shape, and layup

If, besides shape and layup, material becomes an active variable, the pertinent performance index $p=f(M, S, \theta, n)$ is given by Eq.(5). In Fig. 6, this index is plotted for two candidate shapes, the square box and I-beam section, which are the most efficient among the four here examined (Fig. 3), and for two candidate materials, E-Carbon Epoxy (CFRP) and Kevlar (KFRP). The following insight can be gained from Fig 6, where each candidate solutions can be conveniently identified by respecting this format: (M, S, θ, n), which we recall indicate *(material, shape, ply angle ( ), number of plies)*.

(1) If only the angle-ply with $\theta = 0^{\circ}$ and the cross-ply are examined, then the cross-sections can be arranged with decreasing order of stiffness for a given envelope: *(CFRP, Square box, angle-ply); (CFRP, I-beam, angle-ply); (KFRP, Square box, angle-ply); (CFRP, Square box, cross-ply); (KFRP, I-beam, angle-ply); (CFRP, I-beam, cross-ply); (KFRP, Square box, cross-ply); (KFRP, I-beam, cross-ply).*

(2) For a given number of plies, a cross-ply offers the stiffness of the one with the angle ply around ±24°. These apply for all the selected shapes and materials. Hence, other factors, such as shear and torsional stiffness requirements will come into the picture to drive selection. This statement holds for all combinations of shapes and materials.

(3) Consider two cross-sections with $\theta = 0^{\circ}$, one of which is the reference cross-section: *(CFRP, Square box, angle-ply, 16)* and *(CFRP, I-beam, angle-ply, 20)*. It can be seen that the latter is stiffer and lighter, hence an ideal alternative. Another cross-section that has also similar stiffness is *(CFRP, I-beam, angle-ply (10°), 24)*. Despite the similar bending stiffness, it is heavier but possibly has good resistance to shear.

The points reported above show that a number of insights can be obtained from Fig. 6 without the need of numerical calculations. The chart also represents the potential that each material can offer. For instance, by a mere inspection of the domains, one can conclude that on average, KFRP cross-section should be around 0.5 times stiffer

than those in CFRP.

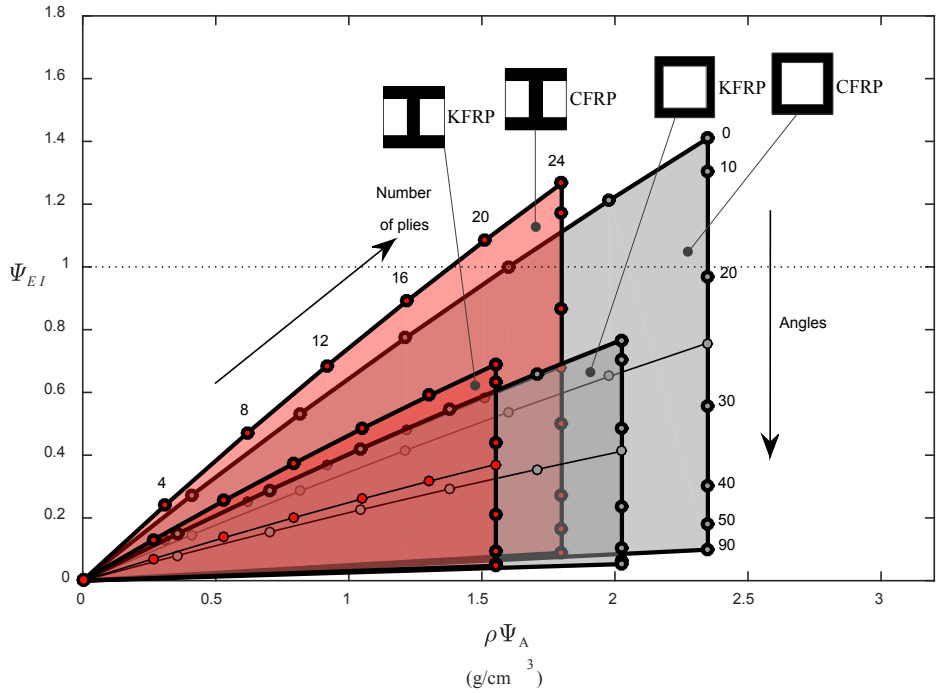

Fig. 6 Design chart for the selection of material, shape, and layup (thin solid lines indicate cross-angle designs)

3.2 Selection charts for maximum bending and torsional stiffness

In this section, we focus our attention on the conflict between bending stiffness and torsion stiffness, and show the extend of this trade-offs by gradually activating the number of variables, starting first with *(S, θ, n)* and then *(M, S, θ, n)*.

3.2.1 Co-selection of shape and layup

To include torsional stiffness in the design charts, we resort to Eq.(7). Similar to the case of conventional materials [18], open cross-sections performs poorly in torsion, as they are several hundred times less stiff. For this reason, this section examines closed cross-sections, leaving open sections in Appendix D.

Fig. 7 shows selection charts for closed cross-sections. For a fixed angle, the stiffness in both bending and torsion increases along with the number of plies. However, from the curves representing a constant number of plies, we observe that the torsional stiffness reaches its peak at 45° as expected, while the maximum bending stiffness is at 0°. Moving from left to right along one of these curves (where the number of plies is fixed), the torsional stiffness firstly increases and then decreases with bending stiffness growing all along. If we divide these curves into two parts with the peak point as divider, there exists an improved design on the right half-curve for each design on the left half-curve. Hence, all the solutions on the left half-curves can be neglected, leaving the bending and torsional stiffness as perfectly antagonist objectives. The right halves of all those curves represent Pareto front solutions. For a constant number of plies, as the angle increases from 0° to 10°, the bending stiffness

decreases and the torsional stiffness increases; however, this change is more evident if the angle increases from 10° to 40°. Hence, a designer might be inclined to choose an angle ply with a lower angle if the bending contribution is more important, or conversely with a higher angle (but smaller than 45°) if the torsion has a heavier weight. The final decision depends upon the designer's preference and design specifications.

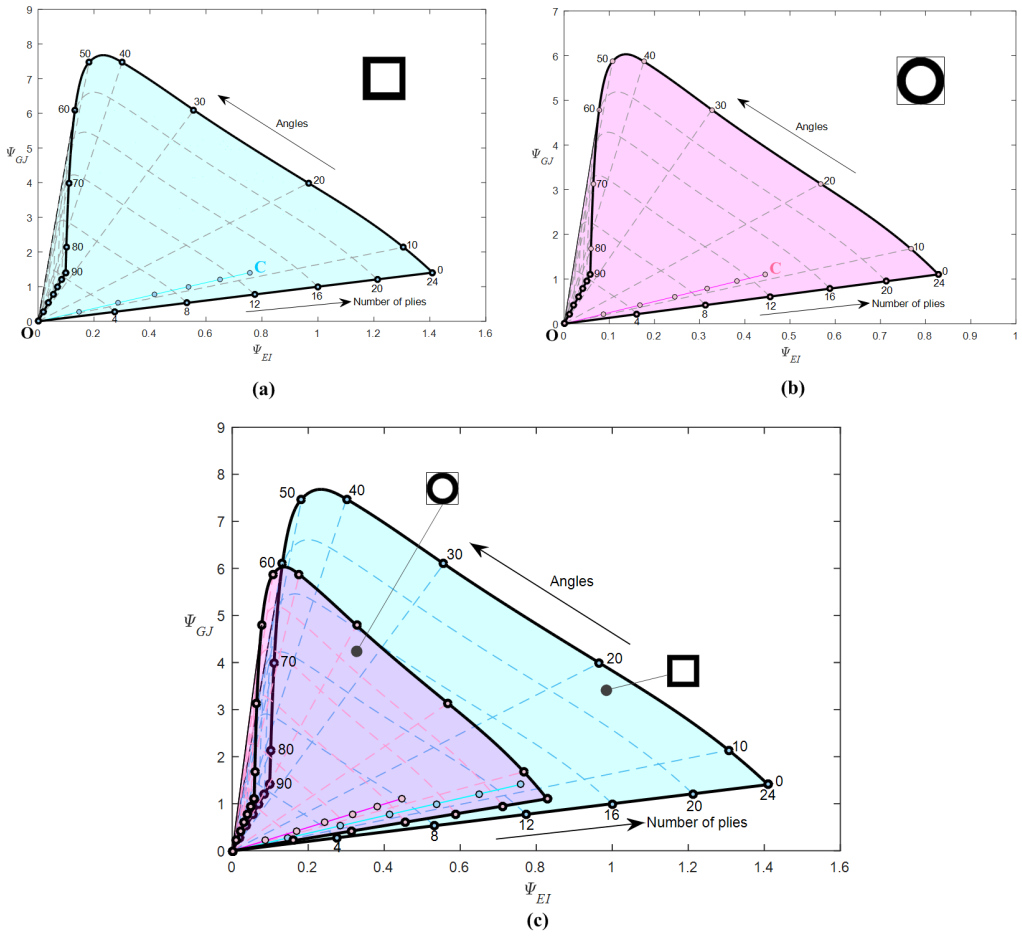

Fig. 7 Co-selection of closed cross-section shape and layup for bending and torsional stiffness. (Cross-angle designs are indicated by thin solid lines, i.e. from O to C)

A general observation to draw from Fig. 7 is that a square box cross-section outperforms a tube one in both torsion and bending. This difference in performance is more manifest at lower angles for bending, and higher angles for torsion. For example, a square box angular laminate with 45° is about 1.25 times stiffer in torsion than their tube counterpart and their bending stiffness is almost identical. On the other hand, a square box angular laminate with 0° is about 1.65 times stiffer in bending than their tube counterpart but their torsional stiffness remains similar. The cross-plies perform poorly in both bending and torsion, whereas they are worse in torsion.

Appendix D reports selection charts for open cross-sections with curves showing similar patterns; hence most of the comments reported above on the angle ply still

hold. In general, an I-beam performs better than a Z-beam, in both bending and torsion.

3.2.2 Co-selection of material, shape, and layup

In this section, we consider *(M, S, θ, n)* as variables of selection. Since displaying the effect of all of them might overcrowd the figure, we illustrate only the boundaries each combination of shape and material can offer. The candidate materials are CFRP and KFRP, and candidates shape are the closed ones (square box and tube in Fig. 3), as open cross-sections are very inefficient in torsion.

Fig. 8 illustrates the relevant domains with that of the CFRP square box cross-section as the most efficient for both torsion and bending. With this combination, a torsional stiffness of about 8 times the reference cross-section or a bending stiffness of 1.4 times the reference cross-section can be achieved. These two are the extreme points, that is, these points should be selected if a designer seeks to maximize one of the stiffness. However, if a designer intends to maximize both the stiffness, relative weights in the formulation of the multi-objective optimization problem can be imparted as proposed in [18]. The negative slopes of each region show the conflicting behavior of the objectives. As discussed in [18], each point on these slopes corresponds to a unique weight factor, which has to be decided by the designer.

In addition, we note that although selection charts for minimum mass and maximum torsional stiffness are not given here, the reader can easily reproduce these charts by using the performance index in Eq.(6). Even though these charts are not presented here, some insight for torsional stiffness can still be observed from the charts for maximum bending and torsional stiffness.

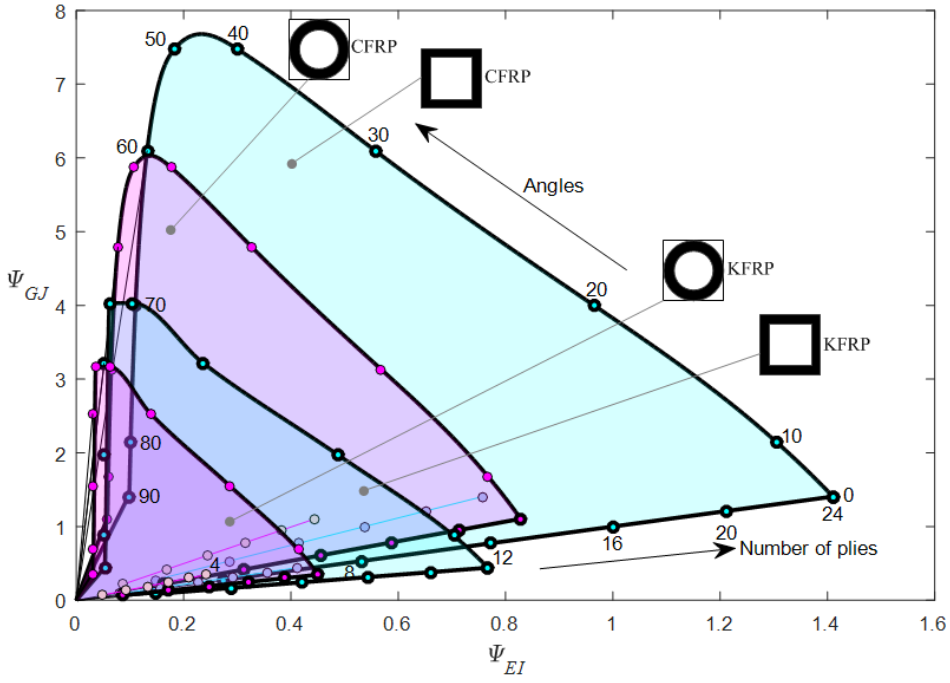

Fig. 8 Chart representing selection domains for combinations of the material, shape, and layup. (thin solid lines indicate cross-angle designs)

4. Selection charts for bending/torsional strength design

In this section we examine the design for strength of a composite laminated beam. As failure criterion for the calculation of the strength, we resort to the Tsai-Wu quadratic interaction criterion, for the others fail to represent the interactions existing in the failure mechanism between the different stress components. Based on the performance indices developed in Section 2.2, we calculate via FEA (MSC.Patran/Nastran, Newport Beach, CA) the strength ratio (*SR*) of the candidate cantilever beam with specified parameters, such as number of plies, angle, cross-section shape and material. By multiplying the values of the applied load (the bending moment, *M*, or the torque, *T*, both of which are assumed to be unity) by SR, we can obtain the critical load (M_f or T_f), for which the beam would fail.

4.1 Selection charts for minimum mass and maximum bending strength

4.1.1 Co-selection of cross-section shape and layup

For given material, the performance index for bending strength design as a function of (S, θ, n) is

$$P = \frac{\Psi_{M_f}}{\Psi_A} \tag{12}$$

Fig. 9 is a plot of the numerator versus the denominator of Eq. (12) for a beam with CFRP square box cross-section in bending strength design. Similarities are readily observed with the selection chart for stiffness selection shown in Fig. 4: the angle increases moving vertically from the top of the triangle to the bottom of the figure. The top boundary of the triangle shows that a square box beam with 0° angle ply performs better than the others with other ply angles for different number of plies. This result is reasonable since the top and bottom walls of a box section undergo the maximum tensile and compressive stress, and most of the composites have different tensile and compressive strengths. They are weaker in the transverse direction, and due to this behavior, the 90° ply angle beams are the worst.

Similarly to stiffness design, consider a case where the performance of a cross-section with number of plies equal to 20 and fiber orientation of ±20°, has to be evaluated and compared to other candidate layups. The chart shows that this candidate cross-section is 0.35 times stronger than the reference and 1.25 times heavier. Additionally, other different designs exist that have the strength equal to that of the reference cross-section, as shown by the horizontal dotted line; yet the reference-cross-section is still the lightest. Depending on the application, a designer may be inclined toward using the design, which has 24 plies at ±10° and has equal collapse load, but a higher mass, which is a trade-off between mass and strength.

In addition, there also exists difference between the selection charts for stiffness and strength. Firstly, for bending stiffness, there is a slight decrease in the stiffness values when the angle varies from 0° to 10°, while a sharp decline from 10° to 40°. A moderate drop appears between 40° and 90°, and the stiffness values do not change too much within this range. However, for bending strength design, sharp decreases

occur from the 0-degree ply, and this phenomenon ends for $\theta = 20^{\circ}$. From 20° to 30°, the bending capacity has a slight drop and since then, the values changes in a small range until $\theta = 90^{\circ}$. Furthermore, as stated in Section 3.1.1, for the performance of a cross-ply laminate with respect to the angle ply, a cross-ply laminate performs equally in bending with the angle ply around 24°, while for the case of bending strength design this occurs for an angle of about 20.5°. Quantitatively, each decrease described above, can be measured from its respective slope. The differences described in this paragraph can also be observed and applied to comment on the other shapes shown in Figs. 10 (a) to 10 (c).

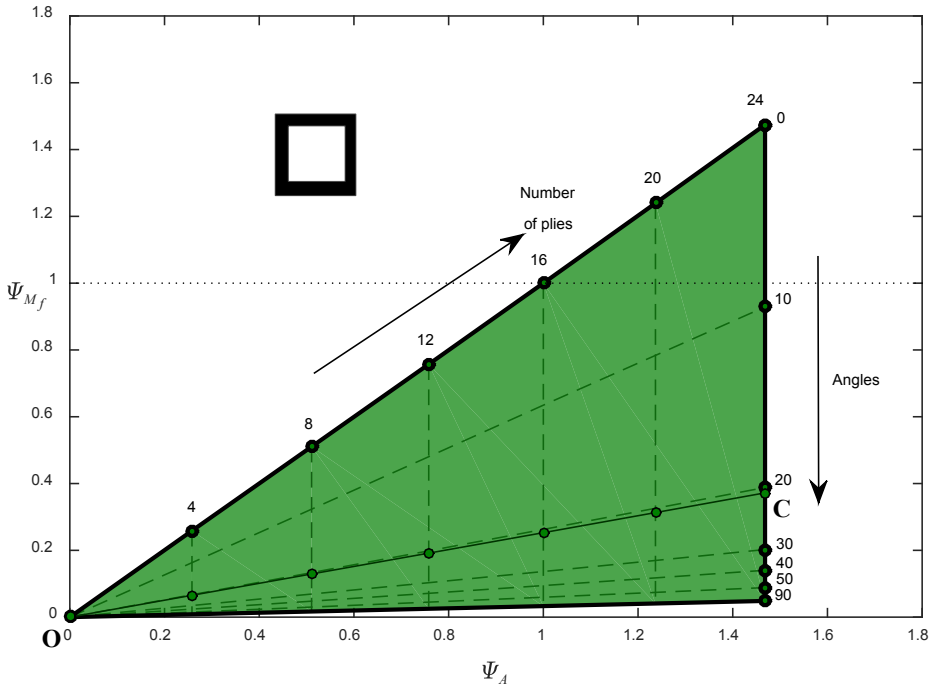

Fig. 9 Bending strength design chart for the selection of ply angle and number of plies for the shape of square box. (Cross-angle designs are shown as a thin solid line, i.e. from O to C)

Fig. 10 visualizes the effects of cross-sectional shape and layup for a CFRP beam of prescribed envelope. Quite similar to the bending stiffness, the I-beam also performs best in bearing the bending moment, as represented by its steepest slope, followed by the square box and tubular sections. On the other hand, differences also exist between the stiffness and strength design charts. Z-beam sections are the most inefficient in bending strength, whereas tubular sections are rather inefficient in stiffness. From Fig. 10, it can also be observed that the boundary of the Z-beam is completely encompassed in that of the tubular beam. Hence, the designer might be inclined to choose a tube cross-section beam with smaller angle if the strength requirement is more important, or a Z-beam if the goal is to reduce mass. Similar comments apply when comparing a tube with a square box section. A simple inspection reveals that if one wishes to replace a square box section with a tubular one, the number of plies should be increased by more than 1.5 times, thereby increasing

the mass by 30%. The final decision is governed by other factors including prescribed design constraints and functional requirements.

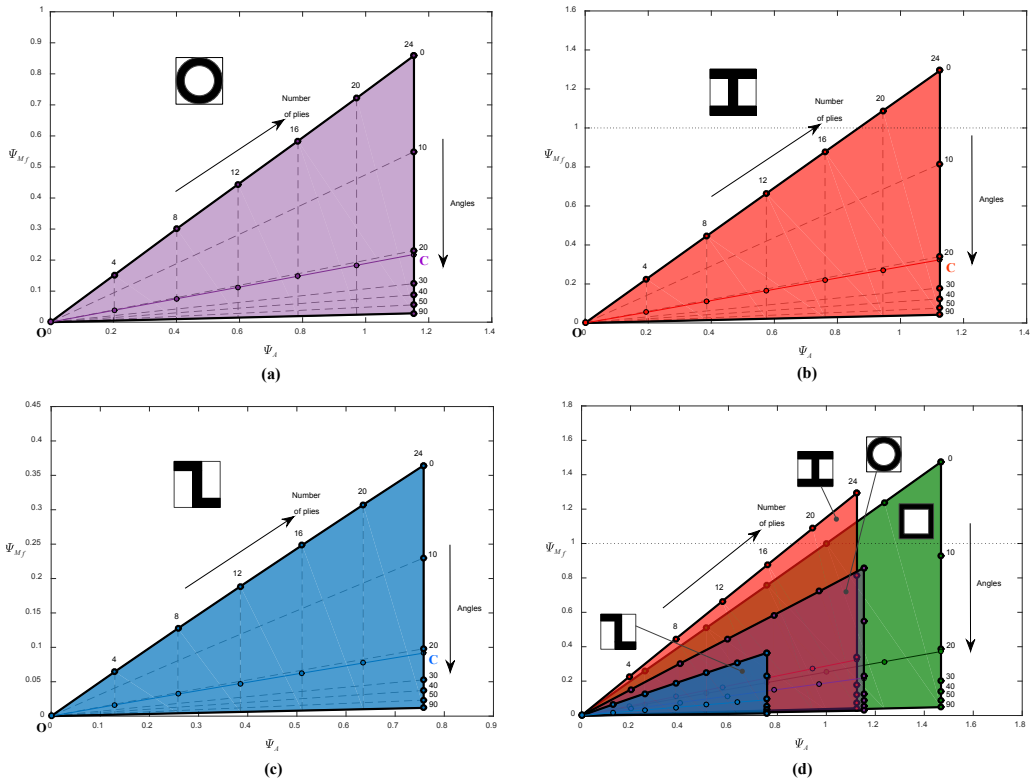

Fig. 10 Bending strength design charts for the selection of shape and layup for a prescribed material. (Cross-angle designs are indicated by thin solid lines, i.e. from O to C)

4.1.2 Co-selection of material, shape, and layup

This section further takes into account the effect of material properties, and corresponding charts are governed by the index in Eq.(8). Similarly to the previous sections, to avoid overcrowding the chart, only the boundaries of each combination are displayed in Fig. 11 for square box and I-beam sections (since these are more efficient as shown in the preceding section), and candidate materials, E-Carbon Epoxy (CFRP) and Kevlar (KFRP).

When considering only the angle-ply with $\theta = 0^{\circ}$ and the cross-ply, the order obtained for stiffness design (Section 3.1.2) cannot be retrieved for strength design. The cross-sections can be ranked in a decreasing stiffness order as: (CFRP, Square box, angle-ply); (CFRP, I-beam, angle-ply); (CFRP, Square box, cross-ply); (CFRP, I-beam, cross-ply) (KFRP, Square box, angle-ply); (KFRP, I-beam, angle-ply); (KFRP, Square box, cross-ply); (KFRP, I-beam, cross-ply). For a given number of plies, a cross-ply has the strength of the one with the angle ply of around ±20.5° for CFRP, while the angle ply is about 15° for KFRP. The boundary for the square box beam with KFRP is located closed to that of the CFRP square box beam. This is similar to the case for the I-beam. Hence, the designer might be inclined to choose a cross-section with a smaller angle made of CFRP if the strength requirement is more

important, or a KFRP-beam if he wants to reduce the mass.

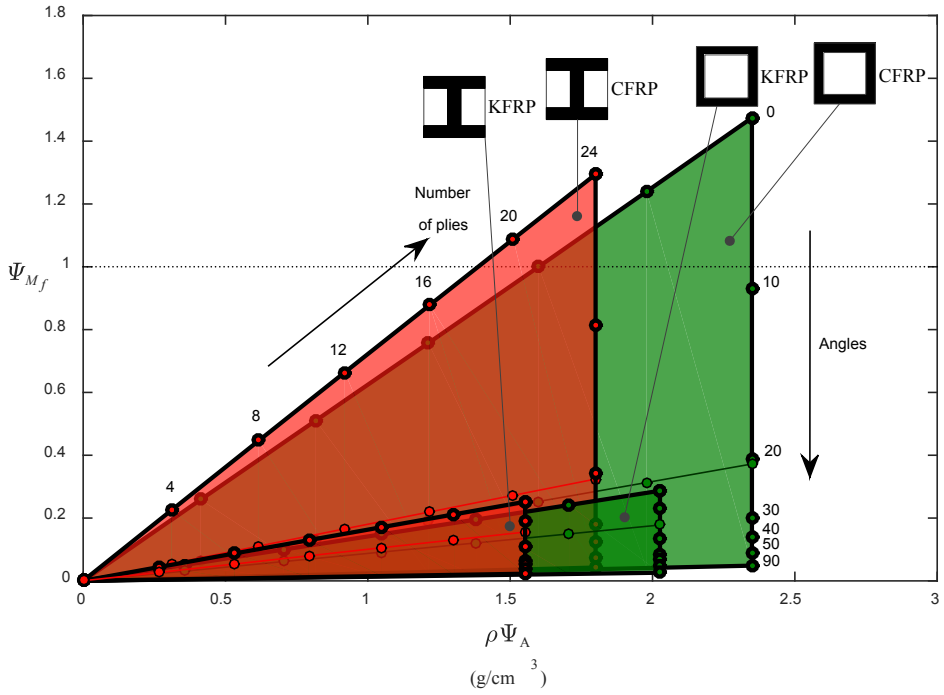

Fig. 11 Bending strength design chart for the co-selection of material, shape, and layup. (Thin solid lines indicate cross-angle designs)

4.2 Selection charts for maximum bending and torsional strength

4.2.1 Co-selection of shape and layup

To take into account torsional strength, Eq.(10) can be used to generate design charts for co-selecting shape and layup bending and torsional strength. Similar to stiffness design, closed sections performs much better than open sections in torsion, and they are dozens of times stronger. Thus, design charts only for closed sections are given in Fig. 12, whereas for open sections in Appendix D.

In Fig. 12, yellow and purple regions represent respectively square box and tubular sections, where dashed lines indicate the angle ply laminates, and solid lines the cross-ply laminates. Similar to stiffness design, the strength in both bending and torsion grows with an increase in the number of plies if the angle is fixed. On the other hand, if the number of plies remains constant, the torsional strength reaches its peak at 45° and the maximum bending strength is at 0°. In strength design, the tendency of these curves is similar to that in stiffness design, as stated in Section 3.2.1. Likewise, when those curves (where the number of plies is given) are dived into two parts by the peak points, all the solutions on the left half-curves can be neglected and the right halves then represent Pareto solutions conflicting in both objectives, i.e. maximizing both bending and torsional strength. On the other hand, if the number of plies is fixed, with the angle ranging from 0° to 20°, the bending strength has a sharp decrease, and this decrease becomes moderate when the angle changes from 20° to 30°, with even less reduction between 30° to 40°. Torsional strength exhibits a

phenomenon that is distinct from that in bending strength. As the angle increases from 0° to 10°, the torsional strength increases moderately; however, this change is more evident when the angle increases from 10° to 40°. A designer might thus be inclined to choose an angle ply with a lower angle if the bending is more important, or with a higher angle for the torsional case.

From Fig.12, it can be obviously observed that a square box cross-section performs better than a tubular one in both torsion and bending strength, and this difference in performance is more manifest at lower angles for bending, and higher angles for torsion, which are cases identical to those in stiffness design. A square box angular laminate with 45° is about 1.15 times stronger in torsion than the tube counterpart while there is not much difference between their bending strength. In addition, a square box angular laminate with 0° is about 1.70 times stronger in bending than their tube counterpart but their torsional strength is similar. Furthermore, the cross-plies perform poorly in both bending and torsion, as is the case in stiffness design.

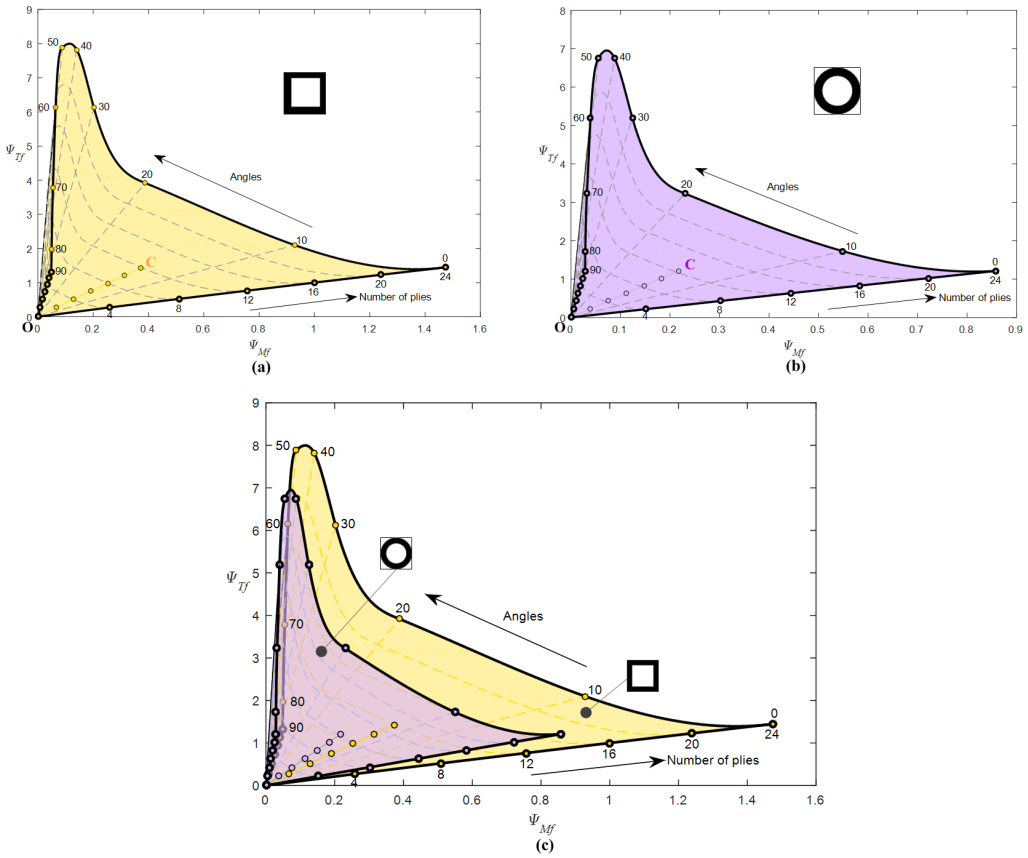

Fig. 12 Co-selection of shape and layup for bending and torsional strength (closed cross-sections). (Cross-angle designs are indicated by thin solid lines, i.e. from O to C)

4.2.2 Co-selection of material, shape, and layup

In this last section, also the material is considered as variable. Candidate materials are CFRP and KFRP, and only closed shapes (square box and tube) are considered. Fig. 13 shows the domain boundaries only for the variable combinations *(M, S, θ, n)*.

Similar to stiffness design, the square box section with CFRP is the most promising. A torsional strength of about 8 times the reference cross-section or a bending strength of 1.5 times the reference cross-section can be obtained, which are the two extreme points. If strength is to be maximized, then one of these two points can be selected. However, if both strengths should be maximum, then relative weights at each objective should be assigned as proposed in [18].

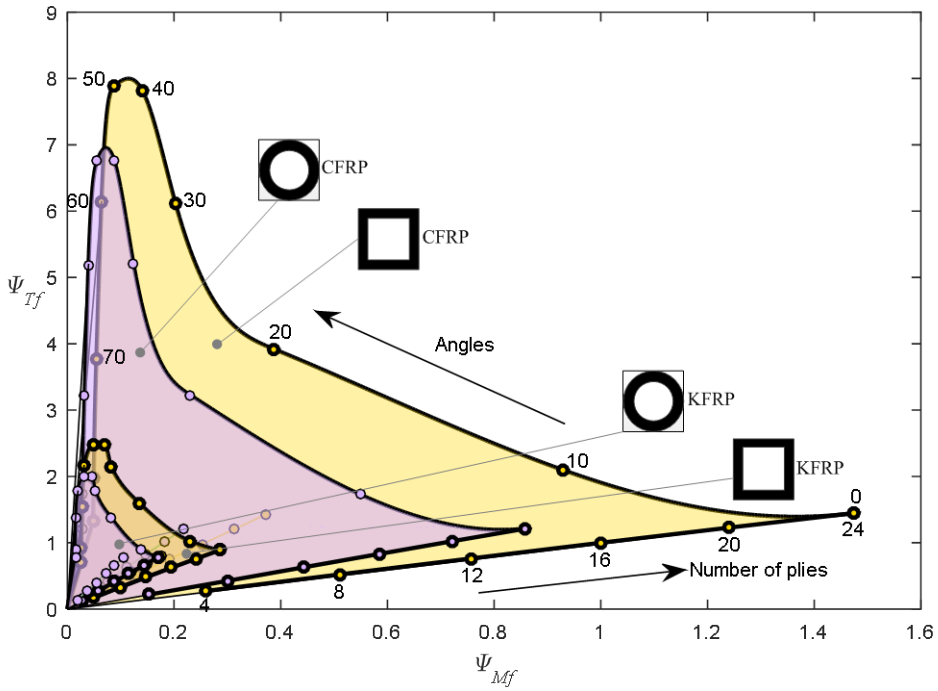

Fig. 13 Design chart representing the potential combination of the material, shape, and layup for bending and torsional strength (thin solid lines indicate the cross-angle designs)

5. Conclusions

The method of shape transformers has been extended in this paper to develop performance indices and to generate design maps for the integrated selection of material, shape and layup in composite laminated structures. Performance indices have been developed for the load cases of bending and torsion in stiffness and strength design, and have been exemplified by generating multiple selection charts that help visualize the interactions between material, shape and layup. From a comparison of closed- and open-walled cross-sections, it appears that the former are much stiffer than the latter in torsion, whereas their bending stiffness performances differ not much. Based on the Tsai-Wu criterion, selection charts for strength evaluation of laminated structures are also presented for bending and torsional cases. Two most prevalent layups, i.e. angle ply and cross ply, can be easily visualized and their performance compared. From both stiffness and strength designs, it can be found that designs with angle ply in small angles are stiffer and stronger than those with cross ply. For angle ply designs, both stiffness and strength decrease for increased angles in bending, whereas they reach their peaks at 45° for torsion. This method provides insight into the optimal selection for laminated composite designs where

numerical methods may prevent designers from visualizing optimal trade-offs among design alternatives. The method can be automated to fill the gap in the well-known Ashby's charts with the addition of layup, which are particularly suitable at the conceptual stage of design.

Acknowledgments
Haichao An acknowledges the support of the China Scholarship Council (Funding No. 201506020070)

Appendix A. Formulation of the performance indices for mass in bending/torsion strength design (conventional solid materials)

Whereas the derivation of the performance indices for bending and torsion stiffness can be found in [16]-[18], here we present those for bending and torsion strength cases since they are unpublished yet. Even though the index for bending strength design was reported in [21], this work only considered solid rectangular cross-sections, whereas herein we consider any types of cross-sections.

Let P_0 be the performance index (mass) for the reference cross-section (solid square). Then, the performance index, P_1 for any arbitrary cross-section with respect to a reference cross-section can be written as

$$\frac{P_1}{P_0} = \frac{m_0}{m_1} = \frac{\rho_0}{\rho_1}\frac{A_0}{A_1} \tag{A.1}$$

In terms of shape transformers and envelope multipliers, it can be expressed as

$$\frac{P_1}{P_0} = \frac{\rho_0}{\rho_1}\frac{A_0}{A_1} = \frac{\rho_0}{\rho_1}\left(\frac{1}{\Psi_A}\frac{1}{uv}\right) \tag{A.2}$$

In bending strength design, both structures are required to meet the same moment failure requirement, M_f, and therefore

$$M_f = \sigma_{f1}Z_1 = \sigma_{f0}Z_0 \tag{A.3}$$

and

$$\frac{\sigma_{f1}}{\sigma_{f0}} = \frac{Z_0}{Z_1} = \frac{{I_0}/{y_{m0}}}{{I_1}/{y_{m1}}} \tag{A.4}$$

where y_m is the furthest distance of the outer fiber from the neutral axis. When the concerned shape is symmetric along the neutral axis, and the centroid is located on the neutral axis, $y_m = h/2$, where h is the height of the envelope. Thus,

$$\frac{\sigma_{f1}}{\sigma_{f0}} = \frac{I_0}{I_1}\frac{h_1}{h_0} = \frac{1}{\Psi_I uv^3}v = \frac{1}{\Psi_I uv^2} \tag{A.5}$$

Rearranging the terms, the bending strength constraint can be written as

$$uv^2 = \frac{1}{\Psi_I}\frac{\sigma_{f0}}{\sigma_{f1}} \tag{A.6}$$

Based on Eq. (A.6), the envelope multipliers, *u* and *v*, can be found

$$u = \left(\frac{1}{\Psi_I}\frac{\sigma_{f0}}{\sigma_{f1}}\right)^{\alpha}, \qquad v = \left(\frac{1}{\Psi_I}\frac{\sigma_{f0}}{\sigma_{f1}}\right)^{\beta} \tag{A.7}$$

where

$$\alpha + 2\beta = 1 \tag{A.8}$$

Finally, the ratio of performance indices can be stated as

$$\begin{aligned}\frac{P_1}{P_0} = \frac{m_0}{m_1} &= \frac{\rho_0}{\rho_1}\frac{1}{\Psi_A}\left(\frac{1}{uv}\right) = \frac{\rho_0}{\rho_1}\frac{1}{\Psi_A}\frac{1}{\left(\frac{1}{\Psi_I}\frac{\sigma_{f0}}{\sigma_{f1}}\right)^{\alpha+\beta}} \\ &= \frac{\rho_0}{\rho_1}\frac{\Psi_{A0}}{\Psi_{A1}}\left(\frac{\Psi_{I1}\sigma_{f1}}{\Psi_{I0}\sigma_{f0}}\right)^{\alpha+\beta}\end{aligned} \tag{A.9}$$

where α and β are obtained by taking logarithm from both sides of Eq. (A.7), and are given by

$$\alpha = \log_{(uv^2)}(u), \quad \beta = \log_{(uv^2)}(v) \tag{A.10}$$

The "$\alpha + \beta$" term in Eq. (A.9) is referred to as the scaling parameter, q. Using Eq. (A.7), the scaling parameter, q, can be expressed in terms of envelope multipliers, *u* and *v*, as

$$q = \alpha + \beta = \log_{(uv^2)}(uv) = \frac{\ln(uv)}{\ln(uv^2)} \tag{A.11}$$

Hence, a unique performance index can be assigned to each cross-section, and can be expressed in terms of material, shape, and size properties as

$$P = \frac{1}{m} = \frac{\left(\Psi_I\sigma_f\right)^q}{\Psi_A\rho} \tag{A.12}$$

When the selectable shapes are limited to solid rectangular cross-sections,$\Psi_I = \Psi_A = 1$, and the performance index becomes

$$P = \frac{1}{m} = \frac{\left(\sigma_f\right)^q}{\rho} \tag{A.13}$$

which is the same with the index derived in [21].

Additionally, for the co-selection of shape and material of a prescribed envelope, the performance index is given as

$$P = \frac{1}{m} = \frac{\Psi_I\sigma_f}{\Psi_A\rho} \tag{A.14}$$

As the envelope is non-scaled, i.e. u=v=1, by rearranging Eq. (A.5) gives

$$\Psi_I \sigma_{f1} = \sigma_{f0} \tag{A.15}$$

Considering the strength requirement in Eq.(A.3), Eq.(A.15) can be expressed as

$$\Psi_I \sigma_{f1} = \sigma_{f0} = \frac{M_f}{Z_0} \tag{A.16}$$

Correspondingly, the co-selection of shape and material for non-scaled cross-sections is governed by the index

$$P = \frac{\Psi_I \sigma_f}{\Psi_A \rho} = \frac{M_f}{Z_0} \frac{1}{\Psi_A \rho} \tag{A.17}$$

With Z_0 as the section modulus of the reference cross-section, which is a constant, the index in Eq.(A.17) can also be given as

$$P = \frac{M_f}{\Psi_A \rho} \tag{A.18}$$

where M_f is the critical failure bending moment of a non-scaled cross-section with optional shapes and materials.

When the approach above is used for torsion strength design, the performance index can be expected to have an expression similar to that in bending strength design, as that in Eq.(A.14). Without detailed derivation process, here we directly give the performance index for mass in torsion strength design

$$P = \frac{1}{m} = \frac{\left(\Psi_{JT} \tau_f\right)^q}{\rho \Psi_A} \tag{A.19}$$

where $q = \ln(uv)/\ln(u^{1.55} v^{1.45})$. For the co-selection of shape and material of a non-scaled envelope, this index can be expressed as

$$P = \frac{1}{m} = \frac{\Psi_{JT} \tau_f}{\Psi_A \rho} \tag{A.20}$$

or

$$P = \frac{T_f}{\Psi_A \rho} \tag{A.21}$$

where T_f is the critical failure torsion torque.

Appendix B. Calculation for the critical bending moment and torsion torque

For the calculation of the critical failure loadings, the first ply failure criterion is used here, and the Tsai-Wu quadratic interaction criterion is employed to evaluate the strength performance. We chose Tsai-Wu criterion since it fully considers the interactions of different stress components in the equations of failure mechanics. The failure index (*FI*) under the Tsai-Wu criterion is written as

$$FI = F_{11}\sigma_1^2 + F_{22}\sigma_2^2 + F_{12}(\sigma_1 \sigma_2) + F_{66}\sigma_{12}^2 + F_1 \sigma_1 + F_2 \sigma_2 \tag{B.1}$$

where σ_1 is the ply longitudinal stress, σ_2 is the ply transverse stress, $\sigma_{12}$is the ply shear stress, and $F_1 = (1/X_T) - (1/X_C)$,$F_2 = (1/Y_T) - (1/Y_C)$, $F_{11} = (1/X_T \cdot X_C)$, $F_{22} = (1/Y_T \cdot Y_C)$, $F_{66} = (1/S^2)$, $F_{12} = -0.5\sqrt{F_{11} \cdot F_{22}}$. For laminated composites,

the Strength Ratio (SR) is a direct failure indicator compared to the Failure Index (FI) which indicates only if failure occurs. Generally, SR is defined as

$$SR = [\sigma] / \sigma \tag{B.2}$$

where $[\sigma]$ is the allowable stress and σ is the calculated stress. For example, a SR=1.2 indicates that the applied loads can be increased by 20% before failure occurs. If we multiply the values of the applied load by this ratio, we can obtain the critical load for which the beam will fail. We now introduce the applied stress as the ratio SR times the applied stress equated to a FI of unity.

$$\begin{aligned} 1.0 = F_{11}SR^2\sigma_1^2 + F_{22}SR^2\sigma_2^2 + F_{12}SR^2(\sigma_1\sigma_2) + F_{66}SR^2\sigma_{12}^2 \\ + F_1SR\sigma_1 + F_2SR\sigma_2 \end{aligned} \tag{B.3}$$

The solutions of this quadratic equation are obtained as

$$SR_1 = \frac{-b + \sqrt{b^2 - 4ac}}{2a} \quad and \quad SR_2 = \frac{-b - \sqrt{b^2 - 4ac}}{2a} \tag{B.4}$$

where

$$a = F_{11}\sigma_1^2 + F_{22}\sigma_2^2 + F_{12}(\sigma_1\sigma_2) + F_{66}\sigma_{12}^2 \tag{B.5}$$

$$b = F_1\sigma_1 + F_2\sigma_2 \tag{B.6}$$

$$c = -1.0 \tag{B.7}$$

The roots of the equation have to be determined, and the positive one is the value of SR. After obtaining SR, by multiplying the values of the applied load by this ratio, the critical load for which the beam fails can be obtained as

$$M_f = M \cdot SR \tag{B.8}$$

$$T_f = T \cdot SR \tag{B.9}$$

Hence, the equations above provide the critical failure loads that are used in Eqs.(24), (25) and (26).

Appendix C. Composite material properties

Table C.1 Properties for the composite materials that are used in this work for demonstrative purposes

Property	**E-Carbon Epoxy (CFRP)**	**Kevlar (KFRP)**
Longitudinal modulus, E_1 [GPa]	147	80
Transverse modulus, E_2 [GPa]	10.3	5.5
Out of plane modulus, E_3 [GPa]	10.3	5.5
In plane shear modulus, G_{12} [GPa]	7.0	2.2
Out of plane shear modulus, G_{23} [GPa]	3.7	1.8
Out of plane shear modulus, G_{13} [GPa]	7.0	2.2
Major in plane Poisson's ratio ν_{12}	0.27	0.34
Out of plane Poisson's ratio ν_{23}	0.54	0.40
Out of plane Poisson's ratio ν_{13}	0.27	0.34
Density, ρ [g/cm^3]	1.60	1.38

Longitudinal tensile strength, F1t [MPa]	2280	1400
Transverse tensile strength, F2t [MPa]	57	30
Out of plane tensile strength, F3t [MPa]	57	30
Longitudinal compressive strength, F1c [MPa]	1725	335
Transverse compressive strength, F2c [MPa]	228	158
Out of plane compressive strength, F3c [MPa]	228	158
In plane shear strength, F6 [MPa]	76	49
Out of plane shear strength, F4[MPa]	39	44
Out of plane shear strength, F5 [MPa]	37	37

Appendix D. Selection charts for bending and torsional stiffness/strength designs of open cross-sections

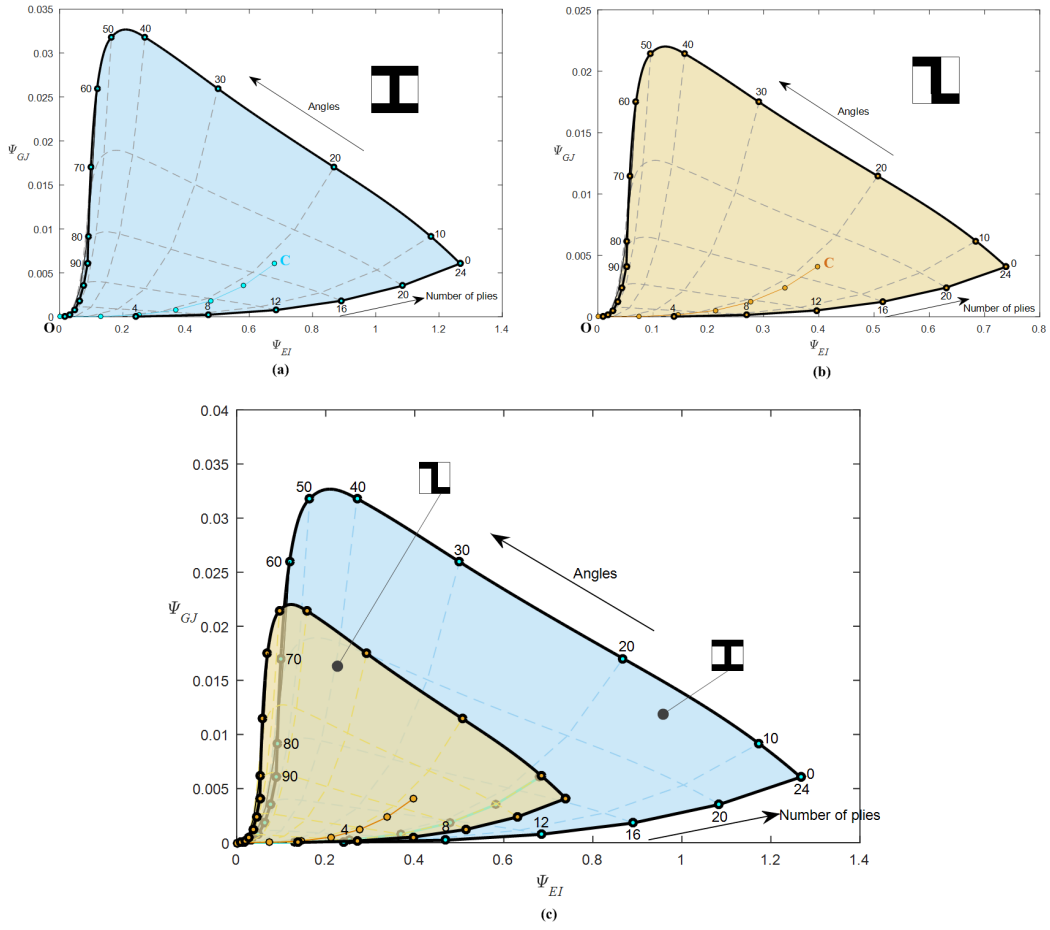

Fig. D.1 Co-selection of shape and layup for bending and torsional stiffness (open cross-sections). (Cross-angle designs are indicated by thin solid lines, i.e. from O to C)

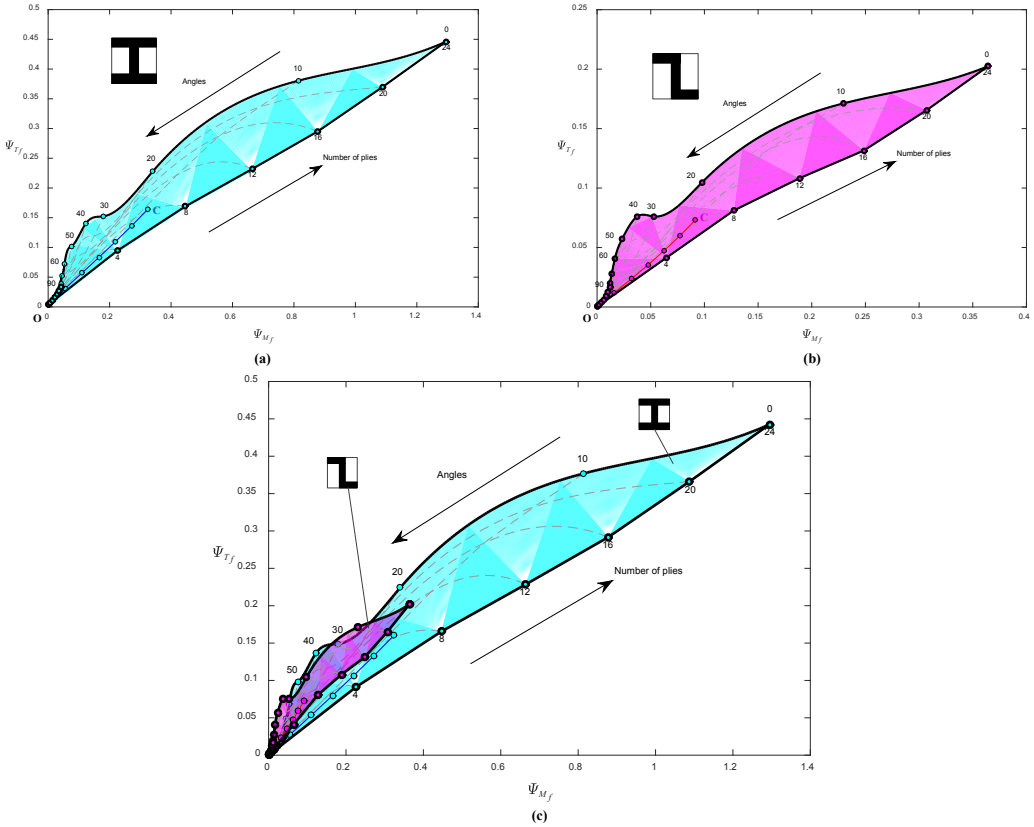

Fig. D.2 Co-selection of shape and layup for bending and torsional strength (open cross-sections). (Cross-angle designs are indicated by thin solid lines, i.e. from O to C)

References

[1] Huang JS, Gibson LJ. Materials and cross-sectional shapes for bending stiffness. Materials Science and Engineering: A, 1993, 163(1): 51-59.

[2] Rakshit S, Ananthasuresh GK. Simultaneous geometry optimization and material selection for truss structures. Proceedings of IDETC/CIE 2006 ASME 2006 International Design Engineering Technical Conferences and Computers and Information in Engineering Conference, September 10-13, 2006, Philadelphia, Pennsylvania, USA. American Society of Mechanical Engineers, pp.1-10.

[3] Wanner A. Minimum-weight materials selection for limited available space. Materials & Design, 2010, 31(6): 2834-2839.

[4] Ashby MF. Materials selection in conceptual design. Materials Science and Technology, 1989, 5(6): 517-525.

[5] Ashby MF. Overview No. 92: Materials and shape. Acta Metallurgica et Materialia, 1991, 39(6): 1025-1039.

[6] Weaver PM, Ashby MF. The optimal selection of material and section-shape. Journal of Engineering Design, 1996, 7(2): 129-150.

[7] Ashby M.F, Bréchet YJM. Designing hybrid materials. Acta Materialia, 2003, 51(19): 5801-5821.

[8] Buckney N, Pirrera A, Weaver PM. Structural Efficiency Measures for Sections Under Asymmetric Bending. Journal of Mechanical Design, 2015, 137(1):

011405-011415.
[9] Thomas JP, Qidwai MA. Mechanical design and performance of composite multifunctional materials. Acta Materialia, 2004, 52(8): 2155-2164.
[10] Bader MG. Materials selection, preliminary design and sizing for composite laminates. Composites Part A: Applied Science and Manufacturing, 1996, 27(1): 65-70.
[11] Weaver PM. Designing composite structures: lay-up selection. Proceedings of the Institution of Mechanical Engineers, Part G: Journal of Aerospace Engineering, 2002, 216(2): 105-116.
[12] Monroy Aceves C, Skordos AA, Sutcliffe MPF. Design selection methodology for composite structures. Materials & Design, 2008, 29(2): 418-426.
[13] Granta Design Limited. Cambridge Engineering Selector CES Edupack 2007. Cambridge, UK.
[14] Monroy Aceves C, Sutcliffea MPF, Ashby MF, Skordos AA, Rodríguez Román C. Design methodology for composite structures: a small low air-speed wind turbine blade case study. Materials & Design, 2012, 36 (April): 296-305.
[15] Pasini D. Shape and material selection for optimizing flexural vibrations in multilayered resonators. IEEE Journal of Microelectromechanical Systems, 2006, 15(6):1745–1758.
[16] Pasini D. Shape transformers for material and shape selection of lightweight beams. Materials & Design, 2007, 28(7): 2071-2079.
[17] Amany A, Pasini D. Material and shape selection for stiff beams under non-uniform flexure. Materials & Design, 2009, 30(4): 1110-1117.
[18] Singh J, Mirjalili V, Pasini D. Integrated shape and material selection for single and multi-performance criteria. Materials & Design, 2011, 32(5): 2909-2922.
[19] Pasini D, Burgess SC, Smith DJ. A method for selecting macro-scale structures with axially loaded members. International Journal of Mechanics and Materials in Design, 2006, 3(2): 185-199.
[20] Pasini D. On the biological shape of the Polygonaceae Rheum Petiole. International Journal of Design & Nature and Ecodynamics, 2008, 3(1): 39-64.
[21] Burgess SC, Pasini D, Smith DJ, Alemzadeh K.A general solution to the material performance index for bending strength design. Materials & Design, 2006, 27(10): 1046-1054.
[22] Kollár LP, Springer GS. Mechanics of Composite Structures. Cambridge University Press, 2003.